Applied Energy 412 (2026) 127666

Contents lists available at ScienceDirect

Applied Energy

journal homepage: www.elsevier.com/locate/apenergy

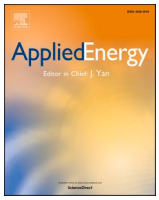

Environmental impacts of fuel cell use in deep-sea shipping towards 2050

Shijie Wei [a,*], Fayas Malik Kanchiralla [b], Henk Polinder [c], Frederik Schulte [c], Arnold Tukker [a,d], Bernhard Steubing [a]

[a] Institute of Environmental Sciences (CML), Leiden University, 2333, CC, Leiden, the Netherlands
[b] Department of Mechanics and Maritime Sciences, Chalmers University of Technology, Hörselgången 4, SE-412 96 Gothenburg, Sweden
[c] Department of Maritime and Transport Technology, Delft University of Technology, Mekelweg 2, 2628, CD, Delft, the Netherlands
[d] Netherlands Organization for Applied Scientific Research TNO, 2595, DA, The Hague, the Netherlands

HIGHLIGHTS

- The cargo capacity change affected by fuel cell propulsion systems is assessed.
- The long-term life cycle environmental impacts of fuel cell use in deep-sea shipping are quantified.
- Fuel cell decarbonization potential in shipping hinges on how clean the hydrogen supply is.
- Fuel cell use in deep-sea shipping can induce new environmental burdens.

ARTICLE INFO

Keywords:
Maritime shipping
Fuel cell
Hydrogen
Ammonia
Climate change
Life-cycle assessment

ABSTRACT

Fuel cells have the potential to reduce greenhouse gas (GHG) emissions from deep-sea shipping. To fully understand the environmental impacts of integrating fuel cells into deep-sea ships, this study evaluates the life cycle environmental impacts from 2020 to 2050 for two leading fuel cell systems: liquid hydrogen with proton exchange membrane fuel cells (liquid-H_2 PEMFC) and liquid ammonia with solid oxide fuel cells (liquid-NH_3 SOFC). The study covers various factors, including changes in cargo capacity, operation modes, developments in hydrogen production and electricity decarbonization. We examine two energy scenarios developed by the International Energy Agency: the Stated Policies Scenario (STEPS) and the Net Zero Emissions by 2050 Scenario (NZE). Our findings reveal that, under different ranges and speeds, the liquid-H_2 PEMFC results in a 2% increase to a 10% decrease in cargo weight, while the liquid-NH_3 SOFC leads to a 4%–23% decrease. By 2050, under the NZE scenario, liquid-H_2 PEMFC and liquid-NH_3 SOFC can reduce GHG emissions per tonne-nautical mile by 69%–75% and 65%–71%, respectively, compared to traditional ships. The use of fuel cells also introduces environmental trade-offs. This assessment can help policymakers gain a more comprehensive understanding of the role of fuel cells in reducing GHG emissions in deep-sea shipping and underscores the potential environmental challenges associated with their large-scale deployment in the future.

1. Introduction

International shipping is crucial to global trade, accounting for over 80% of the merchandise traded between countries [1]. However, the sector's dependence on heavy fuel oil (HFO) and marine gas oil (MGO) in internal combustion engines (ICE) has significant climate change impact. In 2022, international shipping was responsible for about 2% of global energy-related carbon dioxide (CO_2) emissions [2]. Additionally, it emits other pollutants such as nitrogen oxides, sulfur oxides, and particulate matter, which harm both the environment and human health [3,4]. To mitigate the climate change, the International Maritime Organization (IMO) has proposed a target for the shipping industry to achieve net-zero life-cycle greenhouse gas (GHG) emissions by around 2050 [5]. Hydrogen (H_2) and ammonia (NH_3) used with fuel cells have the potential to reduce the hard-to-abate emissions from this sector [6,7].

However, the environmental performance of these emerging decarbonization solutions needs to be assessed from a life cycle perspective.

* Corresponding author.
E-mail address: s.j.wei@cml.leidenuniv.nl (S. Wei).

https://doi.org/10.1016/j.apenergy.2026.127666
Received 8 September 2025; Received in revised form 8 January 2026; Accepted 6 March 2026
Available online 14 March 2026

This is crucial for understanding the technological suitability of these solutions and for defining the most effective implementation pathways [8–10].

Several life cycle assessment (LCA) studies have explored the use of fuel cells on ships. Lee et al. [11] quantified the environmental impacts of a nearshore ferry in South Korea equipped with a proton-exchange membrane fuel cell (PEMFC) using compressed H_2. They found that H_2 produced from natural gas via steam methane reforming results in higher greenhouse gas emissions compared to MGO burned in a diesel generator for the same round trip. Similarly, Hwang et al. [12] compared the environmental impacts of a coastal ferry completing a round trip using either liquid H_2 with a PEMFC or MGO with a diesel engine. They considered H_2 produced from natural gas and liquefied using various electricity sources. Their findings showed that the GHG emissions from using liquid H_2 could be either higher or lower than those from MGO, depending on the electricity source used for H_2 production and liquefaction. Focusing on the fuel origin, Perčić et al. [13] examined the environmental impacts of passenger ships powered by combinations of PEMFC and solid oxide fuel cell (SOFC) systems using liquid H_2 and liquid NH_3 from fossil fuels, carbon capture and storage, and renewables in Croatian coastal waters. The study concluded that fuel cell systems using blue and green H_2 and NH_3 generally have lower environmental impacts compared to diesel-powered ships. Given the potential for a significant influx of new ships powered by alternative fuels and propulsion technologies in the future, Kanchiralla et al. [14] evaluated the environmental impacts of a RoPax ferry (i.e., a vessel that combines passenger cabins with a roll-on/roll-off decks) traveling between Sweden and Germany in 2030, using liquid H_2-PEMFC and liquid NH_3-SOFC, with fuel production sourced from onshore wind. Their results indicated that while these solutions could reduce GHG emissions, they also present environmental trade-offs related to human toxicity and freshwater ecotoxicity associated with wind energy infrastructure. Kanchiralla et al. [15] further compared the environmental impacts of adopting these fuel cell systems across different vessel types, including a RoPax ferry, a tanker, and a service vessel, by 2030.

Existing research primarily focuses on short-sea shipping, leaving a gap in understanding the environmental impacts of fuel cell systems for deep-sea shipping, where GHG emissions are challenging to reduce through direct electrification. In practice, several fuel cell short-sea ships are currently in operation or under construction, despite the considerable cost challenges associated with fuel cell systems [16,17]. With the development of standards and regulations for fuel cells in maritime transportation worldwide, large-scale commercial application and cost reductions may become possible [17]. Additionally, the effects of changes in cargo capacity and energy consumption due to the substitution of propulsion systems have not been systematically explored. Furthermore, factors such as efficiency improvements, regional differences, and the evolving market dynamics of H_2 production over time are overlooked. Broader socio-economic developments also influence the environmental impacts of emerging technologies. To address these gaps, this paper develops life-cycle models for the operation of a typical containership powered by both traditional and fuel cell propulsion systems. These models integrate changes in cargo capacity and energy consumption resulting from the replacement of conventional systems with fuel cell propulsion, along with future global H_2 production and electricity decarbonization scenarios, enabling assessment of the environmental impacts per unit of transport work (the amount of cargo transported over a certain distance) from 2020 to 2050. The main contributions of this paper are twofold. First, the assessment provides valuable insights for deploying fuel cell systems in deep-sea shipping and minimizing their environmental impacts from a long-term perspective. Second, the comprehensive LCA framework developed in this paper lays a foundation for assessing the environmental performance of fuel cell use across the entire shipping sector.

2. Methods and data

The LCA conducted in this study follows the standardized guidelines of ISO 14040: 2006 [18]. The main steps include goal and scope definition, life cycle inventory (LCI) analysis, life cycle impact assessment, and interpretation of results. For the LCI analysis, processes within the system boundary are divided into foreground (see Sections 2.2.1–2.2.6) and background processes (see Section 2.2.7). In the foreground processes, energy, material, and infrastructure inputs as well as emissions are collected from existing literature or calculated. These inventory data are then classified into specific environmental impact categories and the corresponding impacts are quantified using characterization factors.

2.1. Goal and scope

As shown in Fig. 1, this study aims to quantify the cradle-to-grave environmental impacts of operating three types of containerships: one powered by HFO in an ICE, another by liquid H_2 in a PEMFC, and the third by liquid NH_3 in a SOFC. The analysis spans from 2020 to 2050 and is conducted using an attributional LCA approach. The functional unit is the transportation of one tonne of cargo weight over a distance of one nautical mile (t-nm). The analysis focuses on a typical large containership with a capacity of 8749 TEU (20-ft equivalent units). Containerships with a capacity of 8000 to 11,999 TEU were the largest source of GHG emissions in 2018, accounting for 25% of total emissions [19]. They are also projected to have the largest share of the global containership fleet by 2050, reaching up to 20% [19].

To comprehensively assess the impacts of different ship operation modes and broader energy transitions on environmental indicators, this study considers various ship operation scenarios, including range, operation speed (see Section 2.1.1), and future H_2 supply scenarios aligned with different policy settings (see Section 2.2.2). It also incorporates background data reflecting electricity decarbonization under different scenarios (see Section 2.2.7).

2.1.1. Ship design and operation scenarios

Fuel cell propulsion systems vary in both volumetric and gravimetric energy densities, depending on the type of fuel cell and fuel tank used. These variations influence cargo capacity in terms of available space and weight compared to conventional ships. For long-distance vessels, the size of the fuel tank plays a crucial role and is determined by the ship's designed range—a longer range requires a larger tank, which can reduce cargo capacity. Speed also matters, as slower speeds reduce energy consumption for the same range [20], allowing for a smaller fuel tank. Any change in cargo capacity directly affects fuel consumption per transport work, which in turn impacts the ship's environmental performance.

To quantify the environmental impacts of different propulsion system designs and operating conditions, various scenarios covering ship range, operating speed, and refueling frequency are established in this study. As detailed in Table 1, the container ship operates on the Asia-Europe route, specifically between Shanghai and Rotterdam, covering a distance of 11,000 nautical miles. This is one of the main routes for the case ship. The round trip is technically feasible and represents a high fuel demand scenario. Stopping at ports for refueling lowers the amount of fuel that needs to be carried, though increased stops lead to higher operational costs due to port charges and time spent at the dock. A single interim port call is thus assumed to represent the low fuel demand scenario, with the shorter voyage falling within the range of the case ship. Additionally, this study also evaluates results based on an average service speed of 20 nautical miles per hour (i.e., knots) [21] and a reduced speed of 16 knots [22].

2.2. Life cycle inventory analysis

In this section, we present the unit process data for ship production,

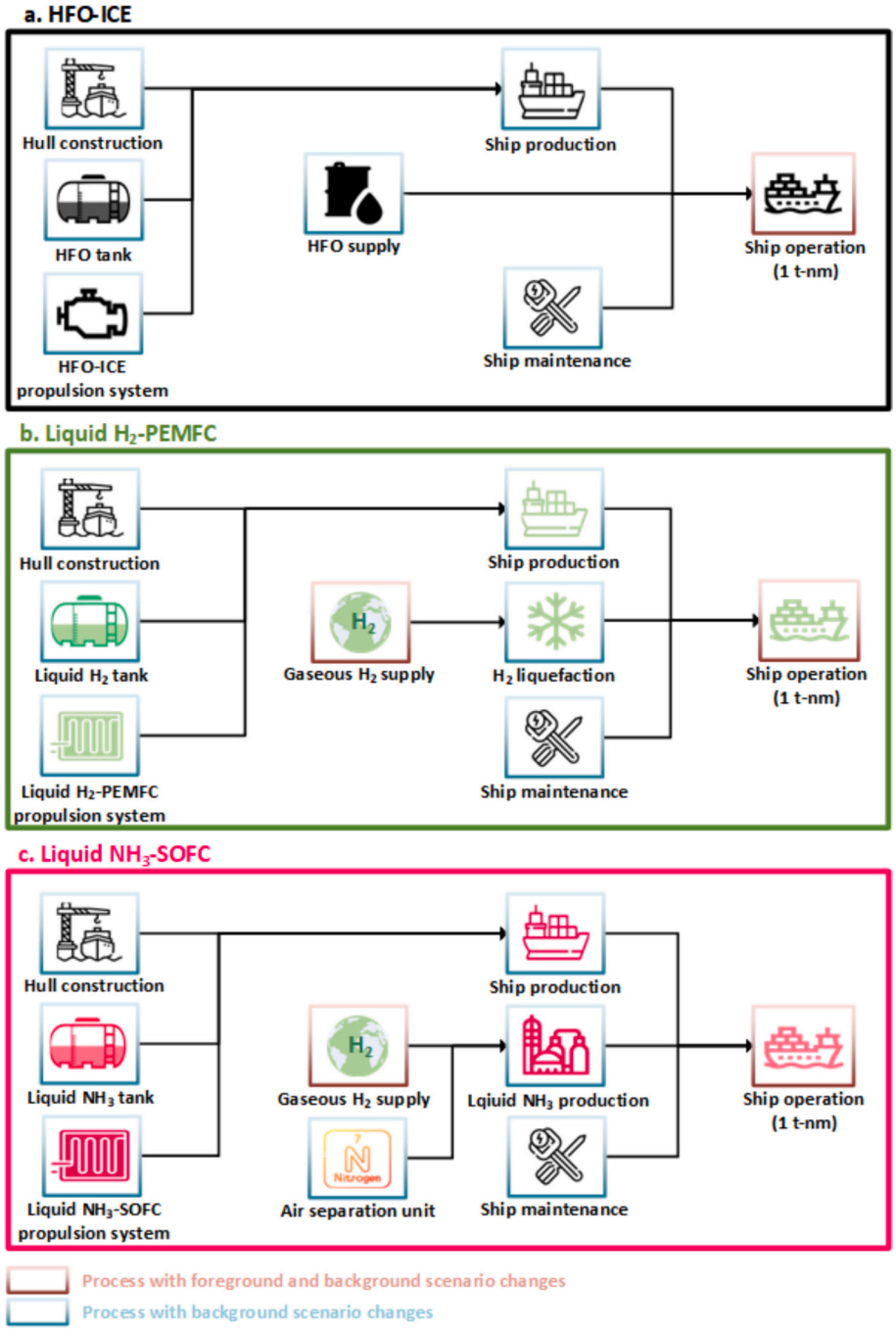

Fig. 1. Simplified system boundaries of container shipping powered by different power systems.

Table 1
Ship design and operation scenarios.

Scenario	R-A-N	R-L-N	S-A-N	S-L-N	S-A-I	S-L-I
Range	22,000 nm	22,000 nm	11,000 nm	11,000 nm	5500 nm	5500 nm
Trip	Return	Return	Single	Single	Single	Single
Speed	20 knots	16 knots	20 knots	16 knots	20 knots	16 knots
Stops to refuel	Nonstop	Nonstop	Nonstop	Nonstop	1	1

fuel supply, and ship operation. Detailed LCI can be found in Section 1 of the Supporting Information (SI).

2.2.1. *Ship construction*

The material composition for constructing the container ship is determined by the lightweight tonnage (LWT), calculated using Eq. 1, and material breakdowns from Jain et al. [23] and Notten et al. [24]. The material demand for the main and auxiliary engines is excluded at this stage, with its detailed LCI collected separately. Welding, electricity, heat usage, and emissions during hull construction are also calculated based on the methodology outlined by Notten et al. [24].

$$LWT = (1-\lambda) \times \frac{DWT}{\lambda} \quad (1)$$

where LWT represents the weight of the empty vessel [25]; deadweight tonnage (DWT) refers to the vessel's load capacity, which includes cargo, fuel, water, crew and their belongings [26], 103800 t [21];

λ is the ratio of DWT to the ship's total weight, 70% [27]. Here, using the HFO ship as a proxy, the LWT (with the weight of the main and auxiliary engines excluded following Jain et al. [23]) is used to estimate the weight of the hull, outfitting and other machinery, hereafter referred to as the hull weight. It is assumed that the ship's hull weight remains constant across ships powered by different propulsion systems. The production of the various propulsion systems is modeled separately, and the differences in weight and volume between the new fuel cell systems and the HFO system affect the cargo capacity.

2.2.2. H_2 supply

The H_2 supply models are taken from our previous study Wei et al. [28]. This study integrates two prospective global H_2 production models from the International Energy Agency: the Stated Policies (STEPS) Scenario and the Net Zero Emissions by 2050 (NZE) Scenario. These models account for nine leading technologies: coal gasification, natural gas steam reforming, biomass gasification (with and without carbon capture and storage (CCS)), and grid-coupled water electrolysis using alkaline electrolyzers, proton exchange membrane electrolyzers, and solid oxide electrolysis cells. The models also take into account electricity decarbonization, efficiency improvements, advancements in electrolyzer technology, and shifts in the H_2 production mix.

2.2.3. HFO and H_2-based fuel supply

Based on the LCI of HFO supply from the ecoinvent database [29], a desulfurization process from Silva [30] is incorporated to reduce the sulfur content in HFO from 1.03% [29] to 0.5%, in order to meet the global sulfur limit outside Sulfur Emission Control Areas (SECAs) mandated by the IMO 2020 regulation [31]. Although HFO with a sulfur content below 0.1% is required within SECAs, fuel switching is not considered in this study, as voyages through these areas account for only a small fraction of the total journey. For the liquid H_2 and NH_3, the LCI of gaseous H_2 from the global market, which represents the weighted average of 15 regional markets, is sourced from Wei et al. [28]. For the production of liquefied H_2, the inputs for the H_2 liquefaction plant and the associated H_2 losses are sourced from Wulf and Zapp [32]. The

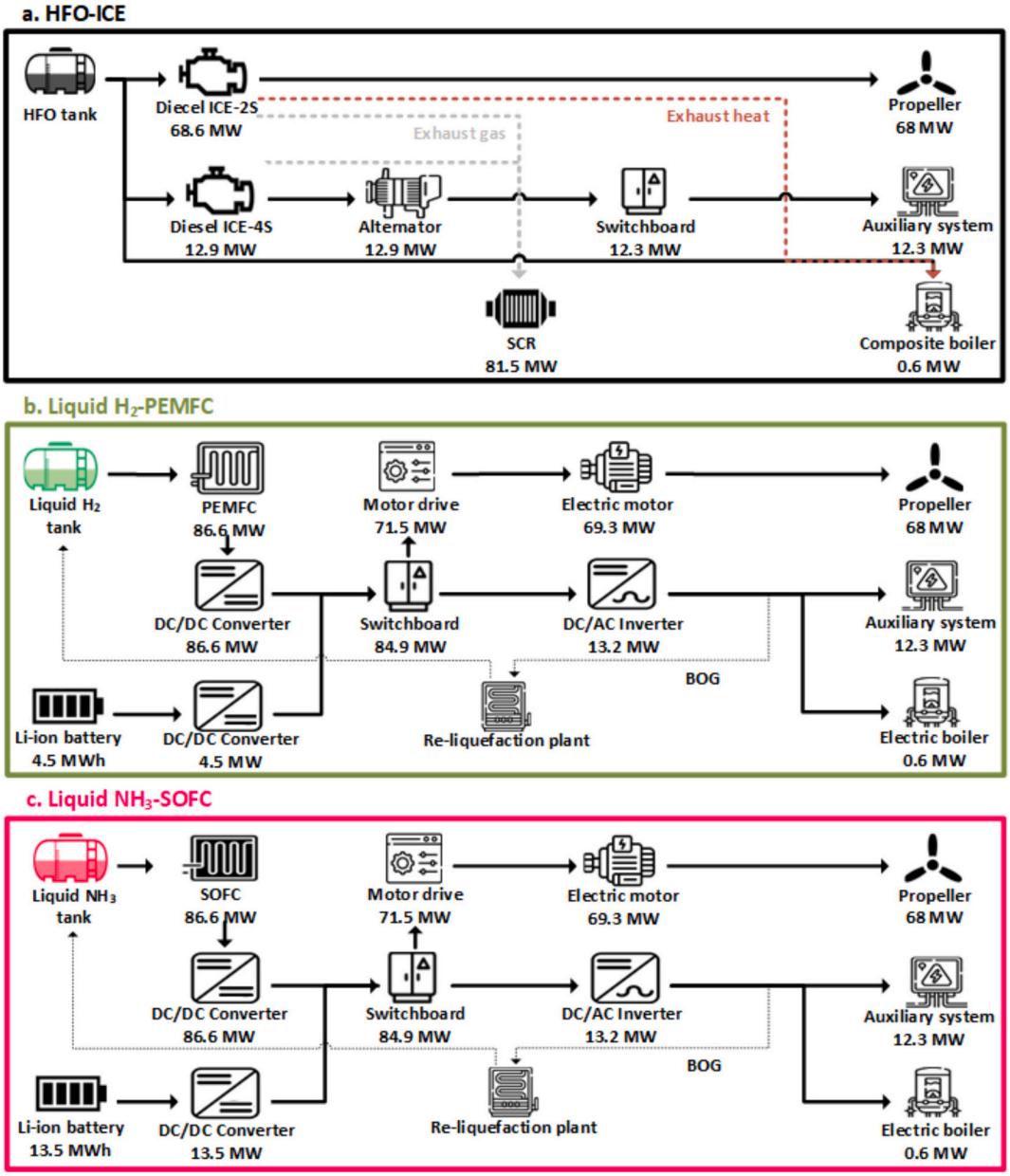

Fig. 2. Components and their dimensions for different propulsion systems.

median electricity consumption of 10.5 kWh to produce one kg liquified H_2 is used [33]. The LCI for liquid NH_3 is taken from D'Angelo et al. [34].

2.2.4. Propulsion systems

The components of traditional and fuel-cell propulsion systems differ substantially, with each system's components sized to deliver equivalent output power to the propeller and auxiliary systems. Fig. 2 shows the workflow, components, and dimensions of HFO-ICE and fuel cell systems. In the HFO-ICE system, the propeller is mechanically driven by a two-stoke diesel ICE. A four-stroke auxiliary ICE is coupled with an alternator to meet the onboard electricity demand. Exhaust gases from both the main and auxiliary ICEs are treated by a selective catalytic reduction (SCR) system to lower nitrogen oxides emissions, ensuring compliance with IMO Tier III regulations. Urea is used as a reducing agent to convert nitrogen oxides into diatomic nitrogen and water [14]. The catalyst in the SCR system, primarily composed of TiO_2, makes up about 0.25% of the SCR's weight [35], and the catalyst must be replaced once during the ship's lifetime [14]. In the HFO-ICE system, a composite boiler is installed to recover the exhaust heat from the main ICE and meet the heat demand. In fuel cell systems, H_2 or NH_3 is directly used to generate electricity through electrochemical redox reactions, which then drive the electric motor and propeller. Since fuel cells supply direct current, it must be converted into alternating current for use in the auxiliary systems and the electric boiler. In fuel cell systems, a battery storage system is included to handle transient operations and provide cold-start power due to the slow response of fuel cells [36]. The battery is sized to support 10 min of operation at 20% load for PEMFCs and 30 min at the same load for SOFCs [15]. This difference reflects the higher operating temperature of SOFCs, which results in slower start-up and response times compared to the lower-temperature PEMFCs [37]. In addition, a reliquefication plant is installed on fuel cell ships to manage boil-off gas (BOG) (see Section 2.2.5 for details). Components such as the PEMFC, SOFC, inverter and battery, which have shorter lifespans than the ship itself, need to be replaced several times over the ship's operational lifetime.

Key parameters and the LCI sources for these components are listed in Table 2. For the LCI related to motor drive manufacturing, material data is sourced from Westberg [38], and electricity consumption data is supplemented from the manufacturer [39].

2.2.5. Fuel storage

The HFO is stored in normal diesel tanks. Liquid H_2 and NH_3 are stored in cryogenic tanks. The properties of these fuels, their storage requirements, and the associated LCI sources are summarized in Table 3.

2.2.6. Ship operation

To complete the same voyage with different propulsion systems and operation scenarios, the corresponding on-board energy demand is determined by the Eq. 2:

$$E_{ij} = \left(\frac{P_{AM_j}}{\eta_{M_i}} + \frac{P_{AA}}{\eta_{A_i}} + \frac{P_{AB}}{\eta_{ABS_i}}\right) \times T_j \times FM \tag{2}$$

whereE_{ij} is the total onboard energy demand for one voyage, given the propulsion system i and operation scenario j, MWh; P_{AM_j}, P_{AA} (as defined in Eq.3–4 [19]) and P_{AB} are the average output power of the main engine under scenario j, the auxiliary engine and the auxiliary boiler, respectively, MW; η_{M_i}, η_{A_i} and η_{ABS_i} represent the efficiencies of the main engine, auxiliary engine and the auxiliary power system i, respectively. In the HFO-ICE system, the auxiliary boiler can utilize exhaust heat, whereas in fuel cell systems, electricity is required to power it; T is the sailing time in hours for operation scenario j, determined by the voyage length and average operating speed; FM is the fuel margin, set at 120% [71].

$$P_{AM_j} = \frac{P_M \times \left(\frac{D_{Ave}}{D_{Max}}\right)^{\frac{2}{3}} \times \left(\frac{S_{Ave_j}}{S_{Max}}\right)^3}{\eta_w \times \eta_f} \tag{3}$$

where P_M is the installed power of the main engine, MW; D_{Max} and D_{Ave} are the maximum and average draught of the ship, respectively; S_{Max} is the maximum operating speed of the ship, and S_{Ave_j} is the average operating speed under scenario j; η_w and η_f denote weather and fouling correction factors (0.867 and 0.917 respectively [19]).

$$P_{AA} = P_A \times LF_A \tag{4}$$

where P_A is the installed power of the auxiliary engine, MW; and LF_A is the average load factor of the auxiliary engine, set at 50% [13].

As liquid H_2 and NH_3 are stored in cryogenic tanks, the boil-off gas (BOG) may occur due to heat ingress. A conservative assumption is made that a reliquefaction process is used to ensure better control and more effective management of BOG [72]. The reliquefaction system is designed based on the maximum hourly BOG volume, and the additional energy required for BOG reliquefaction is calculated using Eq. 5.

$$E_{R_{ij}} = \frac{k_{R_{ij}}}{\lambda_{A_i}} \times \sum_{t=0}^{T-1} \left[\left(\frac{E_{ij}}{\rho_i} - \frac{E_{ij} \times t}{\rho_i \times FM \times T}\right) \times BOG_i\right] \tag{5}$$

where $E_{R_{ij}}$ is the energy demand for reliquefying BOG, in MWh; $k_{R_{ij}}$ is the electricity consumption for reliquefying the BOG of propulsion system i under operation scenario j, assumed as 3.3 kWh/kg for liquid H_2 [73]

Table 2
The key technical parameters of various propulsion systems. In this table, the superscripts in the component column (a, b, c) represent the components required for the HFO-ICE, liquid H_2-PEMFC, and liquid NH_3-SOFC propulsion systems, respectively.

Component	Efficiency (%)	Lifespan (years)	Mass factor (t/MW(h))	Volume factor (m^3/MW(h))	Key parameters source	LCI source
Diesel ICE (Main)[a]	50	25	29.2	27.5	[15,40]	[14]
Diesel ICE (Aux)[a]	48	25	29.2	27.5	[15,40]	[14]
Alternator[a]	96	25	2.5	5.0	[14,40]	[29]
Shafting[a]	99	25	–	–	[41,42]	[24]
SCR[a]	–	25	0.9	5.0	[43,44]	[14]
PEMFC[b]	55	6	3.3	5.7	[15,36]	[45]
SOFC[c]	60	5	45.3	97.2	[15,36]	[15]
Converter (for fuel cell)[b,c]	98	25	2.3	5.1	[46–48]	[29]
Motor drive[b,c]	97	25	1.1	4.4	[49–51]	[38,39]
Electric motor[b,c]	98	25	2.7	4.2	[14,52,53]	[29]
Inverter[b,c]	98	6	3.7	9.0	[54–56]	[29]
Battery[b,c]	96	11	5.9	3.3	[10,36,57]	[29]
Converter (for battery)[b,c]	98	25	3.0	6.7	[36,46,47]	[29]
Switchboard[a,b,c]	99.8	25	0.7	1.4	[58–60]	[24]
Composite boiler[a]	85	25	3	8.8	[61,62]	[29]
Electric boiler[b,c]	99	25	3	8.8	[62,63]	[64]

Table 3
The key technical parameters and data source of various fuels and their storage.

Fuel	Lower heating value (MWh/t)	Gravimetric energy density including tank (MWh/t)	Volumetric energy density including tank (MWh/m^3)	Data source	LCI of fuels	LCI of tanks
HFO	11.9	10.1	10.1	[65]	[29]	[66]
Liquid H_2	33.3	5.6	1.3	[65]	[28,32,33]	[67]
Liquid NH_3	5.2	4.2	2.9	[65,68]	[28,34]	[69,70]

and 0.224 kWh/kg for liquid NH_3 [74]; t is time point of ship operation in one voyage, in hours; ρ_i is the energy density for fuel used in propulsion system i; and BOG_i is the hourly evaporation rate of the fuel used in propulsion system i, assumed as 0.0167% per hour for liquid H_2 and 0.0017% per hour for liquid NH_3 [75].

In addition to the varying volume and mass of fuel and tanks required to meet the energy demands of different propulsion systems, the installed power, volume, and mass of components in fuel cell propulsion systems differ from those in traditional systems. Consequently, these differences lead to changes in cargo space and weight, as shown in Eq. 6 and 7.

$$\Delta V_{ij} = \beta \times V_{OE} + V_{OT} + V_{OO} - \alpha \times V_{FC_i} - \frac{E_{ij} + E_{R_{ij}}}{V_{FT_i}} - V_{FO_i} \tag{6}$$

where ΔV_{ij} represents the change in cargo space change due to the adoption of fuel cell propulsion system i in scenario j, measured in m^3; β is the ratio of the engine room volume to the HFO-ICE main engine volume (V_{OE}), which is 5 times larger due to clearances required for access and maintenance [76]; V_{OT} is the volume of the existing HFO tank, 12000 m^3; V_{OO} is the total volume of other necessary components in the HFO-ICE propulsion system, m^3; α is the ratio of the engine room to the volume of the fuel cell in fuel cell propulsion system i (V_{FC_i}), which is 2 times larger because fuel cells consist of many small modules, significantly reducing the space needed for maintenance and repair [76]; V_{FT_i} is the volumetric energy density of the fuel (including tank) used in the propulsion system i; V_{FO_i} is the total volume of other components in the fuel cell propulsion system i.

$$\Delta M_{ij} = M_{OE} + M_{OT} + \frac{E_{ij}}{G_O} + M_{OO} - M_{FC_i} - \frac{E_{ij} + E_{R_{ij}}}{G_{FT_i}} - M_{FO_i} \tag{7}$$

where the ΔM_{ij} represents the change in cargo weight due to replacing the HFO-ICE propulsion system with the fuel cell propulsion system i in the scenario j, measured in t; M_{OE} is the mass of the HFO main engine; M_{OT} is the mass of the existing HFO tank; G_O is the gravimetric energy density of HFO; M_{OO} is the total mass of other components in the HFO-ICE system; M_{FC_i} is the mass of the fuel cell in the fuel cell system i; G_{FT_i} is the gravimetric energy density of the fuel (including tank) used in the fuel cell propulsion system i; M_{FO_i} is the total mass of other components in the fuel cell propulsion system i.

Finally, the fuel consumption per t-nm is decided by the energy demand leaving the fuel margin, voyage length and resulting cargo weight. The operation parameters corresponding to the fuel used in different propulsion systems are listed in Table 4.

2.2.7. Background scenarios

To address the temporal mismatch between foreground and background data and to account for future developments in key sectors, prospective LCI background databases are used. These are derived from the ecoinvent v3.8 database (system model "Allocation, cut-off by classification") [29] and the latest version of the REMIND model [82], utilizing the open-source Python library premise v1.5.8 [83]. The REMIND model provides global future scenarios based on shared socioeconomic pathways (SSPs) and representative concentration pathways. For the STEPS and NZE scenarios, two prospective LCI databases are employed: SSP2-NDC (projecting approximately 2.5 °C warming by 2100) and SSP1-PkBudg500 (projecting approximately 1.3 °C warming by 2100). These databases include updated electricity inventories, reflecting changes in regional electricity mixes and efficiencies for technologies such as carbon capture and storage, and photovoltaic panels [84].

Table 4
Operation parameters of different propulsion systems.

Propulsion systems	HFO-ICE [77–80]		Liquid-H_2 PEMFC [15]	Liquid-NH_3-SOFC [15]
Engine type	Main engine	Aux engine	PEMFC	SOFC
Specific fuel consumption (g/kWh)	178.6	186.0	54.6	320.5
Urea[a] (g/kWh)	14.4	9.6	–	–
CH_4 (g/kWh)	0.009	0.009	–	–
CO (g/kWh)	0.9	1.0	–	–
CO_2 (g/kWh)	585	605	–	–
NO_x (g/kWh)	3.4	2.6	–	0.003
N_2O (g/kWh)	0.029	0.030	–	–
NH_3 (g/kWh)	0.026	0.026	–	–
NMVOC (g/kWh)	0.424	0.441	–	–
PM_{10} (g/kWh)	0.051	0.053	–	–
$PM_{2.5}$[b] (g/kWh)	0.581	0.605	–	–
SO_2 (g/kWh)	1.795	1.869	–	–

[a] The HFO-ICE is equipped with an SCR unit, using a 40 wt% urea solution to reduce NO_x emissions.
[b] $PM_{2.5}$ is assumed to make up 92% of PM_{10} [81].

LCI modeling and LCA calculations are performed by an open-source software, the Activity Browser [85]. Multiple foreground scenarios and prospective LCI background databases are integrated by the superstructure approach [86].

2.3. Life cycle impact assessment

The climate change impact is quantified based on the IPCC AR5 characterization factors of global warming potentials with a time horizon of 100 years [87]. We add characterization factors for the uptake and release biogenic CO_2 (−1 and + 1 respectively), which is needed to account for technologies such as bioenergy with CCS, and H_2 (+11), as H_2 may leak into the air and act as an indirect greenhouse gas [88]. We also quantify other 15 environmental impacts by the method of Environmental Footprint (EF) v3.0 [89]. The specific information for the environmental indicators is listed in Table 5.

3. Results and discussion

3.1. Cargo space and weight loss

As shown in Fig. 3, the cargo space and weight loss vary depending on the voyage and speed scenarios. Although fuel cell systems have a lower volumetric energy density compared to the HFO-ICE system, the cargo space loss from switching to fuel cell propulsion is relatively minor due to their high energy efficiency. In the S-A-N scenario, both liquid H_2-PEMFC and liquid NH_3-SOFC exhibit similar cargo space losses, at 7% and 4%, respectively. For a round trip, cargo loss can reach up to 20%

Table 5
The specific information for environmental impact categories.

Environmental impact	Unit	Method	Reference
Climate change	kg CO_2-eq	IPCC	[87,88]
Acidification	mol H + -eq	EF v3.0	[89]
Ecotoxicity: freshwater	CTUe	EF v3.0	[89]
Resource use: energy carriers	MJ	EF v3.0	[89]
Eutrophication: aquatic freshwater	kg P-eq	EF v3.0	[89]
Eutrophication: aquatic marine	kg N-eq	EF v3.0	[89]
Eutrophication: terrestrial	mol N-eq	EF v3.0	[89]
Human toxicity: cancer effects	CTUh	EF v3.0	[89]
Human toxicity: cancer effects	CTUh	EF v3.0	[89]
Ionizing radiation: human health	kBq U^{235}	EF v3.0	[89]
Land use	dimensionless	EF v3.0	[89]
Resource use: minerals and metals	kg Sb-eq	EF v3.0	[89]
Ozone depletion	kg CFC-11-eq	EF v3.0	[89]
Particulate matter	disease incidences	EF v3.0	[89]
Photochemical ozone formation	kg NMVOC-eq	EF v3.0	[89]
Water use	kg world eq. deprived	EF v3.0	[89]

and 9% for these two fuel cell systems in the R-A-N scenario, respectively. PEMFCs have a significantly smaller volume and weight compared to ICE and SOFC systems due to their lower operating temperature (80–100 °C) [90]. When interim refueling is available during a voyage, the liquid H_2-PEMFC system leads to negligible cargo space loss in the S-A-I scenario and none in the S-L-I scenario. Although the liquid NH_3-SOFC system can use a smaller tank compared to the HFO-ICE system in the S-A-I and S-L-I scenarios, it still occupies 1% of cargo space because of the lower volumetric density of the SOFC system. It should be noted that although cargo space loss is significant, unlike the cargo weight constraint, it can be alleviated by placing tanks on the deck [91,92].

Across all scenarios, the liquid H_2-PEMFC system results in less cargo weight loss compared to the liquid-NH_3 SOFC system due to its higher gravimetric energy density for on-board storage and lighter fuel cell system. In the R-A-N scenario, liquid H_2-PEMFC and liquid NH_3-SOFC reduce the cargo weight by 10% and 23%, respectively. In general scenarios, such as the S-A-N scenario, the cargo weight capacity with these systems is 2% and 12% lower than that of a traditional ship, respectively. If interim port calls are available during a voyage (S-A-I scenario), the liquid H_2-PEMFC system can increase the cargo weight by 1%, whereas the liquid NH_3-SOFC system results in a 6% reduction in cargo weight. When operating at a lower speed, liquid H_2-PEMFC and liquid NH_3-SOFC systems can reduce cargo weight loss by approximately 1%–4% and 2%–9%, respectively, compared to operating at the average speed.

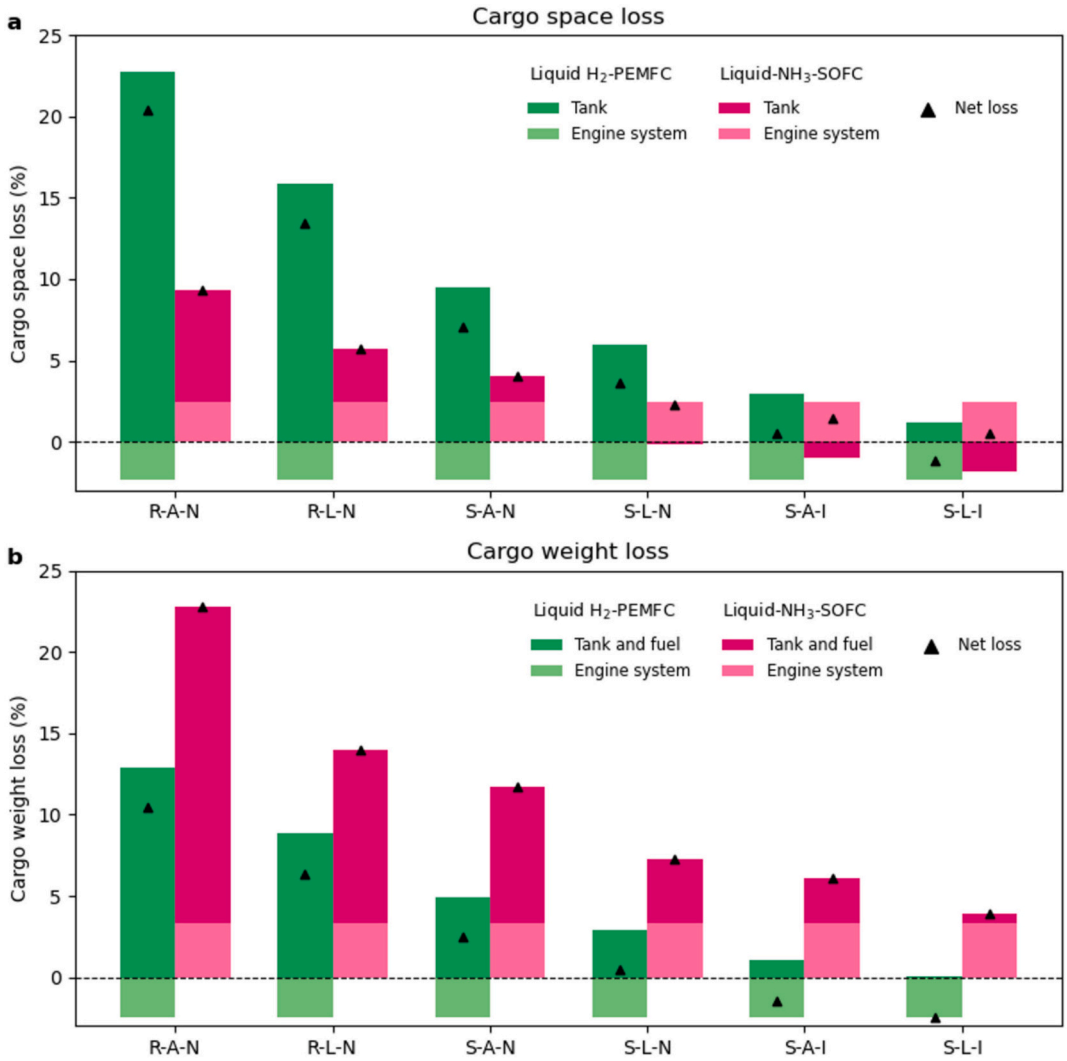

Fig. 3. The cargo space and weight losses associated with fuel cell propulsion systems compared to traditional propulsion systems. In this figure, R-A-*N* = 22,000 nm-20 knots-Nonstop, R-L-N = 22,000 nm-16 knots-Nonstop, S-A-*N* = 11,000 nm-20 knots-Nonstop, S-L-N = 11,000 nm-16 knots-Nonstop, S-A-*I* = 5500 nm-20 knots-1 refueling stop, and S-L-I = 5500 nm-16 knots-1 refueling stop. The net loss is the sum of the loss caused by the tank and fuel, as well as the engine system.

3.2. Global prospective GHG emissions

The prospective GHG emissions of ship transport using traditional ICE versus fuel cell systems are shown in Fig. 4. Currently, fuel cell systems are less effective at decarbonizing deep-sea shipping due to the reliance on fossil fuels, such as natural gas steam reforming and coal gasification, for H_2 production. Additionally, the carbon-intensive electricity used in H_2 liquefaction and liquid NH_3 production significantly contributes to emissions. As a result, the GHG emissions from fuel cell systems are currently about double those of traditional systems. In the STEPS scenario, while electricity decarbonization by 2050 reduces GHG emissions from liquid H_2 and NH_3 production, the H_2 production mix remains largely unchanged, preventing a reduction in overall emissions compared to traditional ships. However, in the NZE scenario, where H_2 production shifts substantially to water electrolysis (61% of the H_2 market) powered by low-carbon electricity by 2050 [93], fuel cell systems can achieve substantial GHG emissions reductions compared with traditional ones. In this scenario, the GHG emissions from fuel cell systems are around 5–8 g CO_2-eq per t-nm. Liquid H_2-PEMFC ships and liquid NH_3-SOFC ships can reduce the GHG emissions by 69–75% and 65–71%, respectively, compared to traditional ships. The liquid H_2-PEMFC system shows slightly lower GHG emissions compared to the liquid NH_3-SOFC system due to the higher gravimetric energy density of liquid H_2 storage and the lighter fuel cell system. Aligning with IMO's 2050 net-zero target, the IMO Net-Zero Framework (NZF), a mandatory regulation, was approved in principle in April 2025. It introduces GHG fuel intensity (GFI) targets requiring ships to reduce their emission intensity on a well-to-wake basis by 4–30% (Tier 2: Base target) and 17–43% (Tier 1: Direct compliance target) during the period 2028–2035, compared with the 2008 reference value of 93.3 g CO_2-eq per MJ. A 2040 base target has also been set, representing a 65% reduction from the reference value [94]. The well-to-wake emissions of fuel cell systems primarily originate from the fuel supply stage. Liquid H_2-PEMFC ships could meet the base and direct compliance targets by 2032 and 2035, respectively, whereas liquid NH_3-SOFC ships could only meet the base target by 2034 (see Table S43 in the SI for detailed data).

Although the use of fuel cell propulsion systems results in a loss of cargo capacity, this is not the primary factor in determining their effectiveness in decarbonizing deep-sea shipping. In the NZE scenario, the GHG emissions from ships powered by fuel cell systems are similar by 2050, regardless of the ranges represented by the R-A-N, S-A-N, and S-A-I scenarios. Even with interim port calls for refueling, the reduction in GHG emissions due to alleviated cargo capacity loss is not significant. Reducing operational speed, as demonstrated in the R-L-N, S-L-N, and S-L-I scenarios, can lead to a decrease in GHG emissions of about 25% for HFO-ICE ships, 19–22% for liquid H_2-PEMFC ships, and 25–31% for liquid NH_3-SOFC ships compared to the average speed by 2050 in the NZE scenario.

In addition to sourcing H_2 from markets, stakeholders in the shipping sector can utilize green H_2 produced from newly established renewable capacities. However, there is significant uncertainty around the supply capacity of green H_2 due to the competing demand for renewable energy. To quantify the potential GHG emissions reduction, we further modeled a scenario with 100% renewable fuel supply. In this case, H_2 is assumed to be produced entirely by PEM electrolyzers powered by onshore wind. The electricity used for H_2 liquefaction and liquid NH_3 production is also sourced from onshore wind. If the entire fuel supply chain is powered by 100% onshore wind, both liquid H_2-PEMFC and liquid NH_3-SOFC ships could achieve the direct compliance GFI target from the start of the NZF's implementation. By 2050, GHG emissions could be reduced by 83–88% for liquid H_2-PEMFC ships and 82–86% for liquid NH_3-SOFC ships compared to HFO-ICE ships. The GHG emissions from fuel cell ships are approximately 2–4 g CO_2-eq per t-nm. Therefore, prioritizing the decarbonization of H_2 production is crucial for reducing GHG emissions in the shipping sector through fuel cell systems. While reducing speed is an effective supplementary strategy, the primary focus should be on transitioning to cleaner H_2 production.

3.3. Regional prospective GHG emissions

The rate of change in H_2 production mix and electricity decarbonization varies across different regions, which affects the GHG emissions from H_2-based fuel supply. To quantify this impact on the GHG emissions of ship operations, this study also models the H_2-based supply in China, the Middle East, and the European Union (EU), where refueling might occur along the case route. Based on the S-A-I scenario, Fig. 5 presents the GHG emissions of fuel cell ships powered by liquid H_2 and NH_3, broken down by H_2 market and various H_2 sources in the three regions mentioned above. As H_2 markets across three regions currently rely on fossil fuels, fuel cell ships in 2020 do not reduce GHG emissions compared to HFO ships, regardless of the refueling location. Their GHG emissions are about 1.3 to 2.5 times higher than those of HFO ships across the three regions. China shows the highest GHG emissions due to its coal-dominated H_2 production and electricity generation mix. The Middle East and the EU have lower GHG emissions, as their H_2 is primarily produced from natural gas. By 2050, in the STEPS scenario, fuel cell ship emissions are expected to decrease mainly due to electricity decarbonization. Although water electrolysis is included in current policies, fossil fuel-based H_2 will still account for at least 87% across three regions. Therefore, decarbonizing ships with fuel cells remains challenging under current policies. Only liquid H_2-PEMFC ships refueled in the EU are expected to slightly reduce GHG emissions compared to HFO-powered ships, primarily due to the lower GHG emissions associated with the electricity and H_2 production mix in that region. In the NZE scenarios, by 2050, fuel cell ships are expected to substantially reduce GHG emissions compared to HFO ships, regardless of refueling location. Although there are regional variations in the H_2 production mix, the GHG emissions from fuel cell ships refueled in different regions are fairly consistent, averaging about one-third of those from HFO ships, at around 6–8 g CO_2-eq per t-nm.

Regarding the GHG emissions of fuel cell ships by H_2 sources, clear regional differences are observed for each H_2 source in 2020. At present, fuel cells powered by fossil fuel-based H_2 such as coal gasification and natural gas steam reforming cannot reduce GHG emissions compared to HFO. This remains true even when fossil fuel-based H_2 production is equipped with CCS, although there is a slight reduction in the EU due to its cleaner electricity mix compared to other regions. At the same time, fuel cells using H_2 from water electrolysis produce 1.8–5.7 times higher GHG emissions than HFO across the three regions, owing to fossil fuel-dominated electricity mixes. Currently, except for China, H_2 from biomass gasification can reduce GHG emissions for fuel cell ships compared to HFO. When biomass gasification is combined with CCS, fuel cell ships can even achieve negative emissions. However, it should be noted that biomass-based H_2 will play only a marginal role in H_2 production even by 2050 [93]. By 2050, the GHG emissions of fuel cells using the same H_2 source become similar across different regions. Under both the STEPS and NZE scenarios, fuel cells using fossil-based H_2 with CCS and those using electrolytic H_2 show significant GHG emissions reductions due to electricity decarbonization. For fuel cells using H_2 from coal gasification and natural gas steam reforming with CCS, emissions could be reduced by 22–48% and 35–57%, respectively, compared to HFO across the three regions in the NZE scenario. Fuel cells using H_2 from water electrolysis present an even greater GHG emissions reduction potential compared to HFO, achieving at least a 74% reduction across the three regions by 2050 in the NZE scenario. Among electrolysis technologies, SOEC exhibits higher GHG emissions compared to AE and PEM due to the additional heat required in H_2 production [28]. These results highlight that ship operations between different regions have varying GHG emissions potential. For fuel cell ship operations, optimizing refueling port selection is key to maximizing GHG emissions reduction potential.

On 1 January 2025, FuelEU Maritime entered into force, setting

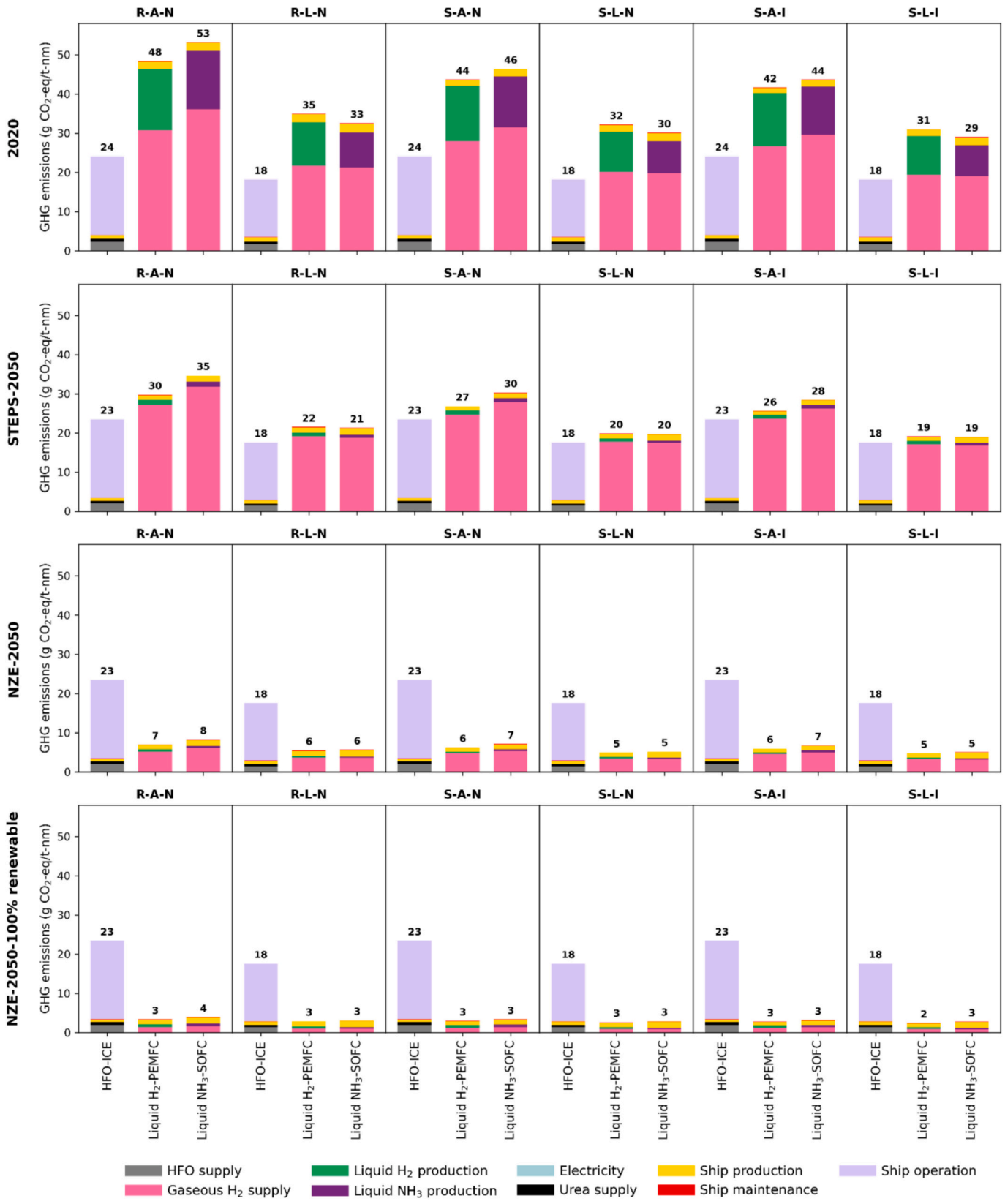

Fig. 4. The process contribution to the GHG emissions of different ships in different scenarios. For the liquid H_2 production and liquid NH_3 production, the gaseous H_2 supply is a part of them and presented separately. In this figure, R-A-*N* = 22,000 nm-20 knots-Nonstop, R-L-N = 22,000 nm-16 knots-Nonstop, S-A-*N* = 11,000 nm-20 knots-Nonstop, S-L-N = 11,000 nm-16 knots-Nonstop, S-A-*I* = 5500 nm-20 knots-1 refueling stop, and S-L-I = 5500 nm-16 knots-1 refueling stop.

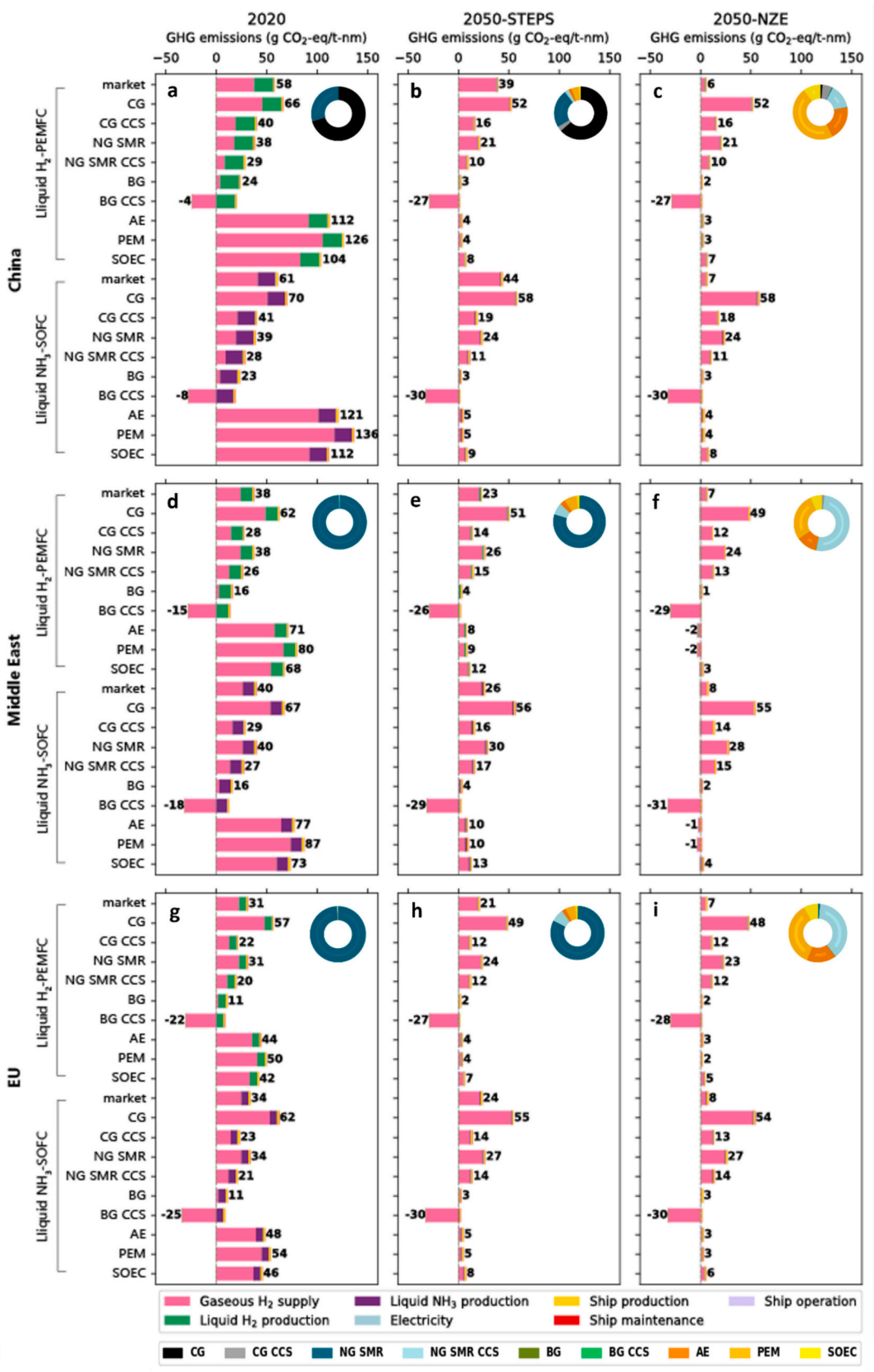

Fig. 5. GHG emissions from ship operations fueled at ports in different regions under the S-A-I scenario (5500 nm-20 knots-1 refueling stop). Subplots a–c show the results for China in 2020, 2050 under the STEPS scenario, and 2050 under the NZE scenario. Subplots d–f show the results for the Middle East, and subplots g–i show the results for the EU. In this figure, the doughnut charts represent the gaseous H_2 production mix for China, the Middle East and the EU. CG = coal gasification, NG SMR = steam methane reforming of natural gas, BG = biomass gasification, CCS = carbon capture and storage, AE = alkaline electrolyzer, PEM = proton exchange membrane electrolyzer and SOEC = solid oxide electrolysis cell.

requirements on the annual average GHG intensity of energy used by ships above 5000 gross tonnage trading within the EU or European Economic Area (EEA). Using 91.16 g CO_2-eq/MJ as the 2020 reference value, the regulation starts with a 2% reduction in 2025, increases to 6% in 2030, and accelerates after 2035 to reach an 80% reduction by 2050 [95]. We further compare the well-to-wake emissions of fuel cells refueled in different regions with FuelEU Maritime requirements (see Table S44 in the SI for detailed data). Based on H_2 market developments in different regions under the NZE scenario, fuel cell ships refueled in China and the Middle East could meet the FuelEU Maritime requirements from 2035, whereas those refueled in the EU could meet the requirements from 2030. However, the presence of fossil fuel-based H_2 with CCS in the market may prevent compliance by 2050. Regarding different H_2 sources, only H_2 from biomass could enable fuel cell ships to meet the requirements consistently from 2025 to 2050. H_2 produced via water electrolysis using AE and PEM technologies could meet the requirements continuously from 2030 to 2050 in the EU, and from 2035 to 2050 in China and the Middle East. Fossil fuel-based H_2 with CCS across

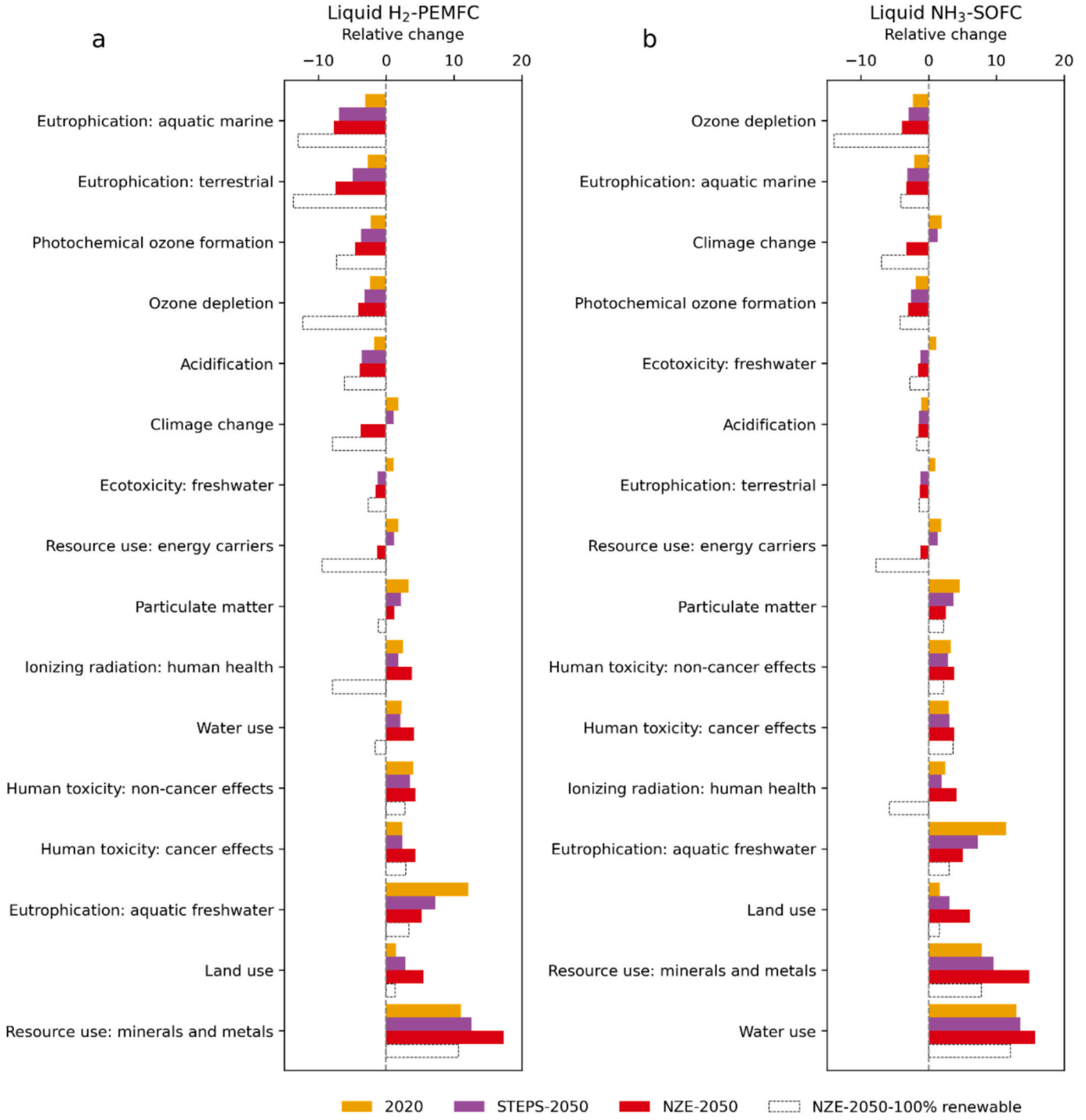

Fig. 6. The relative environmental impacts of fuel cell systems compared to traditional ones from 2020 to 2050 under the S-A-N (11,000 nm-20 knots-Nonstop) scenario. (a) Liquid H_2-PEMFC ship compared under the 2020, STEPS-2050, NZE-2050, and NZE-2050-100% renewable scenarios. (b) Liquid NH_3-SOFC ship compared with the HFO ship under the 2020, STEPS-2050, NZE-2050, and NZE-2050-100% renewable scenarios. The values indicate the factors of change in the environmental impact of fuel cell ships compared to HFO-powered ships.

different regions could help fuel cell ships comply before 2040.

Under the IMO NZF or FuelEU Maritime regulations, the portion of annual average GHG emissions that exceeds the required GFI will incur additional costs, either through the purchase of Remedial Units (RUs) or through penalties, respectively. Under the IMO NZF, the initial RU prices for the reporting periods between 2028 and 2030 are 100 USD/CO_2-eq for Tier 1 compliance deficits and 380 USD/CO_2-eq for Tier 2 [94]. For FuelEU Maritime, the penalty for non-compliance from 2025 is 640 EUR/CO_2-Eq. [96]. In addition, since shipping is covered by the EU Emissions Trading System (EU ETS), companies must purchase sufficient EU allowances by auction to cover all GHG emissions from 2026, with the average allowance price being about 65 EUR/CO_2-eq in 2024 [97,98]. Under the EU ETS, 100% of emissions from voyages and port calls within the EU or EEA and 50% of emissions from voyages into or out of the EU or EEA are subject to compliance [99]. These external costs may accelerate the adoption of fuel cell ships when H_2-based fuels become sufficiently low-carbon. At the same time, the European Commission has launched the European Hydrogen Bank auction that uses emissions trading revenues to support producers of renewable H_2 in the form of a fixed premium [100]. By bridging the gap between renewable H_2 production costs and the price that consumers are willing to pay, the cost of using renewable H_2-based fuels can be further reduced and the potential market for fuel cell ships can be expanded.

3.4. Prospective environmental impacts

Using fuel cell propulsion systems for deep-sea ships can yield both benefits and trade-offs for other environmental indicators. As shown in Fig. 6, in 2020, ships powered by liquid H_2-PEMFC have lower impacts on marine and terrestrial eutrophication, photochemical ozone formation and acidification compared to HFO-ICE ships, due to the absence of nitrogen oxides and sulfur oxides emissions during operation. Additionally, because liquid H_2 production involves fewer hydrocarbons emissions than HFO, the liquid H_2-PEMFC ships also have a lower impact on ozone depletion. The liquid NH_3-SOFC ships offer similar environmental benefits, except for terrestrial eutrophication, due to higher NH_3 and nitrogen oxides emissions during liquid NH_3 production. In the STEPS scenario, as electricity decarbonizes by 2050 with a decline in coal power and its associated emissions of aluminum and nitrogen oxides, environmental benefits extend to reductions in freshwater ecotoxicity for liquid H_2-PEMFC, and to reductions in freshwater ecotoxicity and terrestrial eutrophication for liquid NH_3-SOFC compared to the HFO ship. In the NZE scenario, as electricity and H_2 production become more decarbonized, fuel cell ships are expected to further decrease the aforementioned environmental impacts and fossil fuel use compared to traditional ships by 2050. In a 100% renewable scenario, fuel cell ships can significantly reduce ionizing radiation compared to traditional ships by 2050.

Future fuel cell systems to power ships will continue to face environmental challenges related to minerals and metals use, land use, water use, ionizing radiation, human toxicity, freshwater eutrophication and particulate matter. Fig. S2 further illustrates the contributors to these environmental trade-offs. As the adoption of renewable electricity and water electrolysis expands, some environmental impacts associated with fuel cell ships may worsen. For the minerals and metals use, copper in electricity distribution networks, copper in PEMFCs, and gold in the electronic equipment of liquid NH_3 plants contribute to a higher impact for fuel cell ships compared to traditional ones. In the future, the demand for rare earth metals—such as neodymium, dysprosium, and praseodymium for wind power; tellurium and indium for solar panels; and iridium and platinum for electrolyzers [101,102]—in gaseous H_2 production will become another main driver. For land use, electricity consumption in liquid H_2 and NH_3 production causes fuel cell ships to have a higher impact than traditional ones currently, mainly due to coal-fired electricity and the operation of associated coal mines. In the future, the installation of new infrastructure such as photovoltaic facilities and electrolyzers associated with liquid H_2 and NH_3 supply will significantly increase this impact for fuel cell ships. For water use, coal-dominated electricity in H_2 liquefaction causes liquid H_2-PEMFC ships to have a higher impact compared to the traditional ones. Liquid NH_3-SOFC ships have a higher water use impact compared to liquid H_2 PEMFC ships due to the water cooling requirements in NH_3 production, where evaporation occurs in the water tower. The water use impact of fuel cell ships increases as water electrolysis for H_2 production expands. However, the absolute water consumption for these fuel cell ships is not well-defined and can be assumed to be significantly lower than that of irrigated agriculture. For ionizing radiation, carbon-14 released during the treatment of low-level radioactive waste via plasma torch incineration in petroleum production contributes to the impact associated with HFO ships. For fuel cell ships, this impact is linked to the scale of nuclear power in the electricity mix. As the share of nuclear power decreases in the future, electricity consumption in liquid H_2 and NH_3 production contributes less to this impact. However, gaseous H_2 supply will become the main contributor as the share of water electrolysis in the H_2 market increases. For human toxicity with cancer effects, carcinogenic emissions—such as chromium and hexavalent chromium from low-alloy and stainless steel production for ship structures—are the main contributors. The liquid H_2 and NH_3 tanks lead to a higher impact for fuel cell ships compared to traditional ones. As the share of coal-fired electricity—which also produces hexavalent chromium during hard coal ash treatment—decreases in the electricity mix, the contribution from liquid H_2 and NH_3 production declines. In contrast, the contribution from gaseous H_2 supply increases as water electrolysis expands, due to the substantial demand for steel used in electricity equipment. For human toxicity with non-cancer effects, the main contributors for HFO ships are chloride, lead, and mercury emissions during HFO production, as well as CO emissions during ship operation. For fuel cell ships, intensive electricity use in water electrolysis and PEMFC construction both require large amounts of copper and are associated with lead, arsenic, arsenic ions, and cadmium emissions, thereby worsening human toxicity with non-cancer effects. Nevertheless, the contribution from liquid H_2 and NH_3 processes decreases as coal-fired electricity, which has higher arsenic ion and cadmium emissions, is replaced by renewables.

In contrast, as coal use declines during the energy transition, associated emissions of phosphate and particulate matter smaller than 2.5 μm are also reduced, thereby mitigating freshwater eutrophication and particulate matter formation, respectively. However, the production of copper, steel, multi-silicon wafers, and aluminum for wind turbines and solar panels still generates associated emissions, resulting in higher freshwater eutrophication and particulate matter formation impacts from fuel cell ships compared to HFO-powered ones. The nitrogen oxides and NH_3 emissions during liquid NH_3 production result in a higher particulate matter impact for liquid NH_3-SOFC ships compared to liquid H_2-PEMFC ships, as these emissions can contribute to particulate matter formation [103,104].

The environmental trade-offs of reducing GHG emissions with fuel cell systems are broadly consistent across regions with the global trend, with detailed results provided in Section 2.2 of the SI. It should be noted that results presented for environmental categories not directly related to climate change should not be over-interpreted, as much of the data in this study is focused on GHG emissions. Moreover, technological advancements and waste management strategies to mitigate other environmental impacts were not considered. Our findings aim to highlight areas for further investigation and potential improvement. Finally, we conduct a sensitivity analysis on main parameter assumptions, including fuel cell efficiency, fuel cell lifespan, battery lifespan, and BOG rates of H_2-based fuel on-board storage. The sensitivity analysis shows that improvements in fuel cell efficiency have the greatest impact on all environmental indicators and can be considered an effective way to mitigate the environmental impacts of fuel cell ships. Extending the lifespan of fuel cells shows a low sensitivity for certain environmental indicators, while the impacts of changes in battery lifespan and BOG rates are

negligible (see Section 2.3 in the SI for details).

4. Conclusions

This study quantifies the life cycle environmental impacts of fuel cell-powered ships from 2020 to 2050, examining the effects of cargo capacity changes due to propulsion system replacements, operational modes, and broad energy scenarios. The analysis evaluates the GHG emission reduction potential and other environmental impacts under two future trajectories for global H_2 production technology and mix: the current policy settings (STEPS) and the goal of achieving net zero CO_2 emissions by 2050 (NZE), as outlined by the IEA. The findings provide insights into the potential environmental trade-offs of adopting fuel cells for decarbonizing deep-sea shipping from a long-term perspective, helping policymakers make informed decisions and minimize the environmental impacts of fuel cell ships. The main conclusions are summarized as follows:

The liquid H_2-PEMFC system causes less cargo space loss in short-range operations and consistently results in smaller cargo weight loss for deep-sea ships compared to the liquid NH_3-SOFC system. In various operational modes, the liquid H_2-PEMFC system can either increase cargo space by up to 1% or decrease it by up to 20%. In contrast, the liquid NH_3 SOFC system consistently reduces cargo space by 1% to 9%. When an interim port is available, the liquid-H_2 PEMFC system has a lesser impact on cargo volume compared to the liquid NH_3 SOFC system. Regarding cargo weight, the liquid H_2-PEMFC system can increase it by up to 2% or decrease it by up to 10%, while the liquid NH_3-SOFC system typically results in a decrease of 4% to 23%. Despite the higher energy efficiency of the SOFC, its larger mass and the lower gravimetric energy density of the liquid NH_3 storage system reduce cargo weight more significantly than the liquid H_2-PEMFC system.

Fuel cells can reduce GHG emissions by up to 75% compared to traditional ships by 2050 in the NZE scenario and by 88% in a 100% renewable scenario. Fuel cell ships currently cannot facilitate the decarbonization of deep-sea shipping due to the fossil fuel-dominated energy supply. While lower speeds and interim refueling can somewhat reduce GHG emissions, these measures alone are insufficient to make fuel cell ships have lower GHG emissions compared to traditional HFO-ICE ships. In the STEPS scenario, this remains true by 2050. In the NZE scenario, where H_2 production shifts to water electrolysis powered by low-carbon grid electricity, liquid H_2-PEMFC and liquid NH_3-SOFC ships can reduce GHG emissions by 69%–75% and 65%–71%, respectively, by 2050 compared to HFO-ICE ships. Establishing a 100% renewable fuel supply chain can further enhance their reduction potential to 83%–88% and 82%–86%, respectively. The GHG emissions of fuel cell ships refueled in different regions show significant variations due to different paces of the energy transition. This underscores the critical need to prioritize the decarbonization of H_2 production and to carefully select refueling regions to effectively decarbonize the shipping sector.

The environmental impacts of fuel cell ships should be further minimized. Using fuel cells to decarbonize deep-sea shipping can bring co-benefits by reducing impacts such as marine and terrestrial eutrophication, photochemical ozone formation, ozone depletion, acidification, freshwater ecotoxicity and fossil fuel use compared to traditional ships. However, it also introduces new environmental burdens, including those related to minerals and metals use, water use, land use, freshwater eutrophication, human toxicity, ionizing radiation, and particulate matter. Some of these impacts become more severe as the H_2 production mix shifts to water electrolysis powered by renewables. This calls for comprehensive technological improvements and enhanced waste management measures in the fuel production phase to minimize these environmental impacts.

Fuel cell ships could see gradual adoption after 2030 if H_2 production is sufficiently decarbonized. Achieving substantial GHG emissions reductions from shipping through fuel cell deployment relies on the H_2 market transitioning as rapidly as projected in the IEA's NZE scenario. For H_2 production, scaling up water electrolysis technologies such as AE and PEM electrolysis powered by low-carbon electricity represents a scalable and safer long-term pathway. Under the NZE scenario, and from the perspective of complying with both IMO NZF and FuelEU Maritime regulations, the EU could adopt both liquid H_2-PEMFC and liquid NH_3-SOFC ships from 2030, while China and the Middle East may adopt liquid H_2-PEMFC ships from around 2035. Liquid H_2-PEMFC ships hold an advantage in regulatory compliance due to their lower GHG emissions compared with liquid NH_3-SOFC ships. In addition, policy instruments such as carbon pricing on ship emissions and premiums for renewable H_2 production outside the EU could also be introduced to support the gradual uptake of fuel cell ships.

Future work outlook. In this paper, leading H_2 technologies, as foreseen by the IEA, are used as the basis for producing liquid H_2 and NH_3 and are assessed. Other emerging technologies, such as photocatalytic water splitting (currently with very low conversion efficiency but amenable to scale-up) [105,106] and methane pyrolysis (currently at a low technology readiness level but with potential for rapid expansion) [107], can also be investigated. In addition, this paper focuses on informing policymakers about the future environmental impacts of using fuel cell systems in deep-sea shipping. Further research can examine the economic feasibility of fuel cell shipping by conducting cost comparisons between fuel cell ships and conventional ones. Separate studies could also investigate market acceptance of fuel cell ships.

Declaration of generative AI in scientific writing.

During the preparation of this work the author(s) used OpenAI/ChatGPT in order to polish the language. After using this tool/service, the author(s) reviewed and edited the content as needed and take(s) full responsibility for the content of the published article.

CRediT authorship contribution statement

Shijie Wei: Writing – original draft, Visualization, Methodology, Investigation, Funding acquisition, Formal analysis, Data curation, Conceptualization. **Fayas Malik Kanchiralla:** Writing – review & editing, Methodology. **Henk Polinder:** Writing – review & editing, Methodology. **Frederik Schulte:** Writing – review & editing, Methodology. **Arnold Tukker:** Writing – review & editing, Supervision, Conceptualization. **Bernhard Steubing:** Writing – review & editing, Supervision, Conceptualization.

Declaration of competing interest

The authors declare that they have no known competing financial interests or personal relationships that could have appeared to influence the work reported in this paper.

Acknowledgments

The authors thank the experts for their valuable suggestions that helped refine our analysis. This work is supported by the China Scholarship Council (Grant No. 202006430008).

Appendix A. Supplementary data

Supplementary data to this article can be found online at https://doi.org/10.1016/j.apenergy.2026.127666.

Data availability

The data used in this study are provided in the Supporting Information.

References

[1] UNCTAD. Review of maritime transport 2021. Geneva: United Nations Conference on Trade and Development; 2021.
[2] IEA. Tracking Clean Energy Progress 2023. Paris: International Energy Agency; 2023.
[3] Monteiro A, Russo M, Gama C, Borrego C. How important are maritime emissions for the air quality: at European and national scale. Environ Pollut 2018;242:565–75.
[4] Liu H, Meng Z-H, Lv Z-F, Wang X-T, Deng F-Y, Liu Y, et al. Emissions and health impacts from global shipping embodied in US–China bilateral trade. Nat Sustain 2019;2:1027–33.
[5] IMO. 2023 IMO Strategy on Reduction of GHG Emissions from Ships. International Maritime Organization; 2023.
[6] Müller-Casseres E, Leblanc F, van den Berg M, Fragkos P, Dessens O, Naghash H, et al. International shipping in a world below 2 °C. Nat Clim Chang 2024;14:600–7.
[7] Yang X, Nielsen CP, Song S, McElroy MB. Breaking the hard-to-abate bottleneck in China's path to carbon neutrality with clean hydrogen. Nat Energy 2022;7:955–65.
[8] Fernández-González J, Rumayor M, Domínguez-Ramos A, Irabien A, Ortiz I. The relevance of life cycle assessment tools in the development of emerging decarbonization technologies. JACS Au. 2023;3:2631–9.
[9] Wender BA, Foley RW, Prado-Lopez V, Ravikumar D, Eisenberg DA, Hottle TA, et al. Illustrating anticipatory life cycle assessment for emerging photovoltaic technologies. Environ Sci Technol 2014;48:10531–8.
[10] Stolz B, Held M, Georges G, Boulouchos K. Techno-economic analysis of renewable fuels for ships carrying bulk cargo in Europe. Nat Energy 2022;7:203–12.
[11] Lee G, Kim J, Jung K, Park H, Jang H, Lee C, et al. Environmental life-cycle assessment of eco-friendly alternative ship fuels (MGO, LNG, and Hydrogen) for 170 GT nearshore ferry. J Mar Sci Eng 2022;10:755.
[12] Hwang S, Gil S, Lee G, Lee J, Park H, Jung K, et al. Life cycle assessment of alternative ship fuels for coastal ferry operating in Republic of Korea. J Mar Sci Eng 2020;8:660.
[13] Perčić M, Vladimir N, Jovanović I, Koričan M. Application of fuel cells with zero-carbon fuels in short-sea shipping. Appl Energy 2022;309:118463.
[14] Kanchiralla FM, Brynolf S, Malmgren E, Hansson J, Grahn M. Life-cycle assessment and costing of fuels and propulsion systems in future fossil-free shipping. Environ Sci Technol 2022;56:12517–31.
[15] Kanchiralla FM, Brynolf S, Olsson T, Ellis J, Hansson J, Grahn M. How do variations in ship operation impact the techno-economic feasibility and environmental performance of fossil-free fuels? A life cycle study. Appl Energy 2023;350:121773.
[16] Wang Z, Dong B, Wang Y, Li M, Liu H, Han F. Analysis and evaluation of fuel cell technologies for sustainable ship power: energy efficiency and environmental impact. Energy Conversion and Management: X. 2024;21:100482.
[17] Fu Z, Lu L, Zhang C, Xu Q, Zhang X, Gao Z, et al. Fuel cell and hydrogen in maritime application: a review on aspects of technology, cost and regulations. Sustain Energy Technol Assess 2023;57:103181.
[18] ISO. ISO 14040. 2006.
[19] IMO. Fourth Greenhouse Gas Study 2020. London: International Maritime Organization; 2021.
[20] Lindstad H, Asbjørnslett BE, Strømman AH. Reductions in greenhouse gas emissions and cost by shipping at lower speeds. Energy Policy. 2011;39:3456–64.
[21] Scheepvaartwest. Colombo Express - IMO 9295244. Scheepvaartwest.be. 2020.
[22] MI. What is The Speed of a Ship at Sea? Marine Insight. 2019.
[23] Jain KP, Pruyn JFJ, Hopman JJ. Quantitative assessment of material composition of end-of-life ships using onboard documentation. Resour Conserv Recycl 2016;107:1–9.
[24] Notten PJ, Althaus H-J, Burke M, Läderach A. Life cycle inventories of global shipping - Global. Zürich: Ecoinvent Association; 2018.
[25] Eyres David J. Ship Construction. Oxford. UK: Published by Elsavier Ltd. Departement; 2007.
[26] Tupper EC. Chapter 2 - Definition and Regulation. In: Tupper EC, editor. Introduction to Naval Architecture (Fifth Edition). Oxford: Butterworth-Heinemann; 2013. p. 9–32.
[27] Papanikolaou A. Ship Design - Methodologies of Preliminary Design. 2014.
[28] Wei S, Sacchi R, Tukker A, Suh S, Steubing B. Future environmental impacts of global hydrogen production. Energy Environ Sci 2024;17:2157–72.
[29] Wernet G, Bauer C, Steubing B, Reinhard J, Moreno-Ruiz E, Weidema B. The ecoinvent database version 3 (part I): overview and methodology. Int J Life Cycle Assess 2016;21:1218–30.
[30] Silva M. Life Cycle Assessment of Marine Fuel Production. Trondheim: Norwegian University of Science and Technology; 2017.
[31] IMO. The 2020 global sulphur limit. International Maritime Organization; 2021.
[32] Wulf C, Zapp P. Assessment of system variations for hydrogen transport by liquid organic hydrogen carriers. Int J Hydrogen Energy 2018;43:11884–95.
[33] Al Ghafri SZS, Munro S, Cardella U, Funke T, Notardonato W, Trusler JPM, et al. Hydrogen liquefaction: a review of the fundamental physics, engineering practice and future opportunities. Energy Environ Sci 2022;15:2690–731.
[34] D'Angelo SC, Cobo S, Tulus V, Nabera A, Martín AJ, Pérez-Ramírez J, et al. Planetary boundaries analysis of low-carbon ammonia production routes. ACS Sustain Chem Eng 2021;9:9740–9.
[35] Liang Z, Ma X, Lin H, Tang Y. The energy consumption and environmental impacts of SCR technology in China. Appl Energy 2011;88:1120–9.
[36] Kim K, Roh G, Kim W, Chun K. A preliminary study on an alternative ship propulsion system fueled by ammonia: environmental and economic assessments. Journal of Marine Science and Engineering 2020;8:183.
[37] U.S.DOE. Comparison of Fuel Cell Technologies. Washington, DC: U.S. Department of Energy; 2016.
[38] Westberg E. Environmental Impact of an Electric Motor and Drive : Life Cycle Assessment and a study of a Circular Business Model. Linköping: Linköping University. 2020.
[39] ABB. ACS 6000 Medium Voltage AC drive for speedand torque control for power of 3 MW to 27 MW motors. Zurich: ABB; 2003.
[40] MAN-ES. Marine engine programme-2nd edition 2023. Augsburg: MAN Energy Solutions; 2023.
[41] MAN-ES. Basic principles of ship propulsion. Copenhagen: MAN Energy Solutions; 2018.
[42] Guellec C, Doudard C, Levieil B, Jian L, Ezanno A, Calloch S. Parametric method for the assessment of fatigue damage for marine shaft lines. Mar Struct 2023;87:103325.
[43] Zhao Y, Fan Y, Fagerholt K, Zhou J. Reducing sulfur and nitrogen emissions in shipping economically. Transp Res D Transp Environ 2021;90:102641.
[44] Shih-Tung S. A Life Cycle Cost Analysis of Marine Scrubber Technologies. Rostock: University of Rostock; 2013.
[45] Usai L, Hung CR, Vásquez F, Windsheimer M, Burheim OS, Strømman AH. Life cycle assessment of fuel cell systems for light duty vehicles, current state-of-the-art and future impacts. J Clean Prod 2021;280:125086.
[46] IISB F. High Power SiC DC/DC Converters. Erlangen: Fraunhofer Institute for Integrated Systems and Device Technology. 2014.
[47] PPS. Railway and Industry 2000W DC/DC Converter. PREMIUM POWER SUPPLIES. 2024.
[48] ABB. Solar Inverters—ABB Medium Voltage Compact Skid (PVS-175-MVCS). Zurich: ABB. 2019.
[49] GEPC. MV6 Medium Voltage Drive-Leading next generation technology. Paris: GE Power Conversion; 2017.
[50] RA. PowerFlex 7000 Medium Voltage AC VFD—Air-Cooled. Milwaukee: Rockwell Automation; 2024.
[51] ABB. Medium Voltage AC Drive ACS 5000, 1.5 MW–36 MW, 6.0–6.9 kV. Zurich: ABB; 2013.
[52] Grzesiak S. Alternative propulsion plants for modern LNG carriers. New Trends Prod Eng 2018;1:399–407.
[53] HE. Induction Motors Medium & High Voltage. Seongnam-si: Hyundai Electric; 2019.
[54] Tazelaar E. Energy management and sizing of fuel cell hybrid propulsion systems. Eindhoven: Technische Universiteit Eindhoven; 2013.
[55] GPhilos. FUEL CELL INVERTER. 2024.
[56] ABB. Central Inverters—PVS800, 100 to 1000 kW. Zurich: ABB; 2014.
[57] Ellingsen LA-W, Majeau-Bettez G, Singh B, Srivastava AK, Valøen LO, Strømman AH. Life cycle assessment of a lithium-ion battery vehicle pack. J Ind Ecol 2014;18:113–24.
[58] MAN-SE. Diesel-electric Propulsion Plants: A brief guideline how to engineer a diesel-electric propulsion system. Munich: MAN Energy Solutions; 2012.
[59] EPD. Switchboard Maintenance: Safeguarding Your Electrical System's Longevity. Electronic Power Design. 2024.
[60] SIEMENS. Air-Insulated Medium-Voltage Switchgear NXAirS, up to 12 kV. 2020.
[61] SPIRAX SARCO. Boiler Efficiency and Combustion. 2024.
[62] PARAT. Marine Boilers. Flekkefjord. 2024.
[63] BOSCH. Electric steam boiler ELSB. 2025.
[64] Abbas AMA. Life Cycle Assessment of Water Heating Systems Used in Health Clubs. Nablus: An-Najah National University; 2015.
[65] TNO. E-fuels: Towards a more sustainable future for truck transport, shipping and aviation. Delft: Netherlands Organisation for Applied Scientific Research. 2020.
[66] Dlamini NG, Fujimura K, Yamasue E, Okumura H, Ishihara KN. The environmental LCA of steel vs HDPE car fuel tanks with varied pollution control. Int J Life Cycle Assess 2011;16:410–9.
[67] Abbas EWM. Life Cycle Assessment of Hydrogen Storage Systems for Trucks - An Assessment of Environmental Impacts and Recycling Flows of Carbon Fiber. Gothenburg, Sweden: Chalmers University of Technology; 2022.
[68] EMSA. Potential of Ammonia as Fuel in Shipping. Lisbon: European Maritime Safety Agency. 2022.
[69] Ryste JM. Screening LCA of GHG emissions related to LNG as ship fuel. Trondheim: Norwegian University of Science and Technology; 2012.
[70] Cryocan. Ammonia Storage Tank. 2014.
[71] ICCT. Refueling Assessment of a Zero-Emission Container Corridor between China and the United States: Could Hydrogen Replace Fossil Fuels. Washington, DC: International Council on Clean Transportation. 2020.
[72] McKinlay CJ, Turnock SR, Hudson DA. Route to zero emission shipping: hydrogen, ammonia or methanol? Int J Hydrogen Energy 2021;46:28282–97.
[73] Lee H, Shao Y, Lee S, Roh G, Chun K, Kang H. Analysis and assessment of partial re-liquefaction system for liquefied hydrogen tankers using liquefied natural gas (LNG) and H_2 hybrid propulsion. Int J Hydrogen Energy 2019;44:15056–71.
[74] Lee J, Choi Y, Choi J. Techno-economic analysis of NH_3 fuel supply and onboard re-liquefaction system for an NH_3-fueled ocean-going large container ship. J Mar Sci Eng 2022;10:1500.
[75] Song Q, Tinoco RR, Yang H, Yang Q, Jiang H, Chen Y, et al. A comparative study on energy efficiency of the maritime supply chains for liquefied hydrogen, ammonia, methanol and natural gas. Carbon Capture Science & Technology 2022;4:100056.

[76] Minnehan JJ, Pratt JW. Practical Application Limits of Fuel Cells and Batteries for Zero Emission Vessels. United States: Sandia National Laboratories; 2017.
[77] Kanchiralla FM, Brynolf S, Mjelde A. Role of biofuels, electro-fuels, and blue fuels for shipping: environmental and economic life cycle considerations. Energy Environ Sci 2024;17:6393–418.
[78] Tan ECD, Hawkins TR, Lee U, Tao L, Meyer PA, Wang M, et al. Biofuel options for marine applications: technoeconomic and life-cycle analyses. Environ Sci Technol 2021;55:7561–70.
[79] Andersson K, Winnes H. Environmental trade-offs in nitrogen oxide removal from ship engine exhausts. Proceedings of the Institution of Mechanical Engineers, Part M: Journal of Engineering for the Maritime Environment. 2011;225:33–42.
[80] EGCSA. NOx Reduction by Exhaust Gas Recirculation – MAN explains. 2014.
[81] IMO. Fourth IMO GHG Study 2020. London: International Maritime Organization; 2021.
[82] Baumstark L, Bauer N, Benke F, Bertram C, Bi S, Gong CC, et al. REMIND2.1: transformation and innovation dynamics of the energy-economic system within climate and sustainability limits. Geosci Model Dev 2021;14:6571–603.
[83] Sacchi R, Terlouw T, Siala K, Dirnaichner A, Bauer C, Cox B, et al. PRospective EnvironMental Impact asSEment (premise): a streamlined approach to producing databases for prospective life cycle assessment using integrated assessment models. Renew Sustain Energy Rev 2022;160:112311.
[84] Lamers P, Ghosh T, Upasani S, Sacchi R, Daioglou V. Linking life cycle and integrated assessment modeling to evaluate technologies in an evolving system context: a power-to-hydrogen case study for the United States. Environ Sci Technol 2023;57:2464–73.
[85] Steubing B, de Koning D, Haas A, Mutel CL. The activity browser — an open source LCA software building on top of the brightway framework. Softw Impact 2020;3:100012.
[86] Steubing B, de Koning D. Making the use of scenarios in LCA easier: the superstructure approach. Int J Life Cycle Assess 2021;26:2248–62.
[87] IPCC. Climate Change 2013 – The Physical Science Basis: Working Group I Contribution to the Fifth Assessment Report of the Intergovernmental Panel on Climate Change. Cambridge: Intergovernmental Panel on Climate Change; 2013.
[88] Warwick N, Griffiths P, Keeble J, Archibald A, Pyle J, Shine K. Atmospheric implications of increased Hydrogen use. London: Department for Energy Security & Net Zero and Department for Business. Energy & Industrial Strategy 2022.
[89] Fazio S, Biganzioli F, De Laurentiis V, Zampori L, Sala SD. E. Supporting information to the characterisation factors of recommended EF Life Cycle Impact Assessment methods, Version 2, from ILCD to EF 3.0. Ispra: European Commission. 2018.
[90] Hwang SS, Gil SJ, Lee GN, Lee JW, Park H, Jung KH, et al. Life cycle assessment of alternative ship fuels for coastal ferry operating in Republic of Korea. J Mar Sci Eng 2020;8:660.
[91] ABS. Setting the Course to Low Carbon Shipping: View of the Value Chain. Texas: American Bureau of Shipping; 2021.
[92] IEA-AMF. Alternative Fuels for Marine Applications. Wieselburg: International Energy Agency-Advanced Motor Fuels; 2013.
[93] IEA. Net Zero by 2050. International Energy Agency; 2021.
[94] DNV. IMO Net-Zero Framework. Det Norske Veritas; 2025.
[95] DNV. FuelEU Maritime. Det Norske Veritas; 2025.
[96] OceanScore. FuelEU Maritime Compliance: Why Pooling Is Infinitely Better Than Paying the Penalty. 2025.
[97] ICAP. EU Emissions Trading System (EU ETS). Berlin: International Carbon Action Partnership; 2025.
[98] EC. Reducing emissions from the shipping sector. European Commission. 2025.
[99] DNV. EU ETS – Emissions Trading System. Det Norske Veritas; 2025.
[100] EC. Commission launches first European Hydrogen Bank auction with €800 million of subsidies for renewable hydrogen production. European Commission. 2023.
[101] Luderer G, Pehl M, Arvesen A, Gibon T, Bodirsky BL, de Boer HS, et al. Environmental co-benefits and adverse side-effects of alternative power sector decarbonization strategies. Nat Commun 2019;10:5229.
[102] Bareiß K, de la Rua C, Möckl M, Hamacher T. Life cycle assessment of hydrogen from proton exchange membrane water electrolysis in future energy systems. Appl Energy 2019;237:862–72.
[103] Gu B, Zhang L, Van Dingenen R, Vieno M, Van Grinsven HJM, Zhang X, et al. Abating ammonia is more cost-effective than nitrogen oxides for mitigating PM2.5 air pollution. Science 2021;374:758–62.
[104] Jin X, Behrens P, Erisman JW, Mogollón JM. Ammonia emissions from agricultural products at high resolution across Europe. Sci Data 2025;12:1493.
[105] Nishiyama H, Yamada T, Nakabayashi M, Maehara Y, Yamaguchi M, Kuromiya Y, et al. Photocatalytic solar hydrogen production from water on a 100-m^2 scale. Nature 2021;598:304–7.
[106] Zhou P, Navid IA, Ma Y, Xiao Y, Wang P, Ye Z, et al. Solar-to-hydrogen efficiency of more than 9% in photocatalytic water splitting. Nature 2023;613:66–70.
[107] Moghaddam AL, Hejazi S, Fattahi M, Kibria MG, Thomson MJ, AlEisa R, et al. Methane pyrolysis for hydrogen production: navigating the path to a net zero future. Energy Environ Sci 2025;18:2747–90.

Glossary

AE: Alkaline electrolyzer
BG: Biomass gasification
BOG: Boil-off gas
CCS: Carbon Capture and Storage
CG: Coal gasification
CO_2: Carbon dioxide
DWT: Deadweight tonnage
EEA: European Economic Area
EF: Environmental Footprint
EU: European Union
EU ETS: EU Emissions Trading System
GHG: Greenhouse gas
GFI: GHG fuel intensity
HFO: Heavy fuel oil
H_2: Hydrogen
ICE: Internal combustion engines
IMO: International Maritime Organization
LCA: Life cycle assessment
LCI: Life cycle inventory
LWT: Lightweight tonnage
MGO: Marine gas oil
NG SMR: Steam methane reforming of natural gas
NH_3: Ammonia
NZE: Net Zero Emissions by 2050 Scenario
NZF: IMO Net-Zero Framework
PEM: Proton exchange membrane electrolyzer
PEMFC: Proton exchange membrane fuel cell
SCR: Selective catalytic reduction
SECAs: Sulfur Emission Control Areas
SOEC: Solid oxide electrolysis cell
SOFC: Solid oxide fuel cell
SSPs: Shared Socioeconomic Pathways
STEPS: Stated Policies Scenario
TEU: 20-ft equivalent units